Turbulence closure modeling near rigid boundaries

By P. A. Durbin

1. Motivation and objectives

The near-wall region plays an essential role in turbulent boundary layers: it is a region of high shear; the peak rate of production and peak intensity of turbulence occurs there; and the peak rate of dissipation occurs right at the wall. Nevertheless, this region has received less attention from modelers than have more nearly homogeneous flows. One reason for this is that when the boundary layer is near equilibrium, experimental data can be used to prescribe the flow in the wall layer. Another reason is that most turbulence models are developed under assumptions of near homogeneity. This is a poor approximation in the wall region. My objective has been to develop a single-point moment closure model for the strongly non-homogeneous A turbulent flow near a rigid boundary.

All the previous work in this area has used an eddy viscosity 'damping function' (this is true of second order closures as well as of k–ϵ models). The need for a damping function in k–ϵ models is explained by figure 1. The solid curve is the exact eddy viscosity

$$\nu_t = -\overline{uv}/\partial_y U \tag{1}$$

evaluated from DNS data. The dotted curves are the k–ϵ viscosity

$$\nu_t = C_\mu k T \tag{2}$$

where $T = k/\epsilon$ (see §2.3 below). The standard value of $C_\mu = 0.09$ is used in the upper curve while $C_\mu = 0.075$ in the lower. One sees that in the wall region ($y_+ < 100$) the k–ϵ viscosity has the wrong profile. A damping function is commonly used to correct this fundamentally wrong behavior; the damping function is simply defined as the ratio of the solid to the dotted curve.

Tensoral considerations (Lumley 1978) suggest that

$$\nu_t = C_\mu \overline{v^2} T \tag{3}$$

might be a more basically correct form. The dashed line shows that this, with $C_\mu = 0.2$, is a good approximation when $y_+ < 100$. Of course, figure 1 was constructed using DNS data for k, ϵ and $\overline{v^2}$; what is required is a model which can predict these quantities.

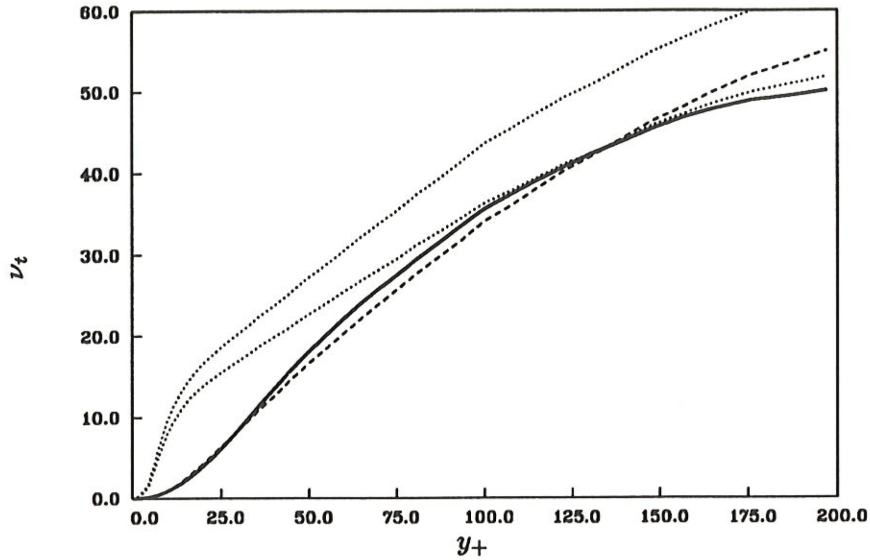

FIGURE 1. Exact eddy viscosity (solid) compared to k–ϵ (dotted, $C_\mu = 0.09$ upper, $C_\mu = 0.075$ lower) and k–ϵ–v (dashed) formulas. These curves were computed from DNS data.

2. Accomplishments

2.1. Near wall model

Such a model has been developed and is described in Durbin (1990). In this section, the model will be described very briefly.

Boundary conditions are important in near wall modeling. The no-slip and no-normal flux conditions lead to

$$\begin{aligned} k = \partial_y k &= 0 \\ \overline{v^2} &= O(y^4) \end{aligned} \tag{4}$$

at the boundary, $y = 0$. In order to satisfy these conditions at the two boundaries to a channel, the model equations must be fourth order. The standard k–ϵ system has this property. In the thin-layer approximation with an eddy viscosity model for turbulent transport, the standard k–ϵ system is

$$\begin{aligned} \partial_y(\nu + \nu_t/\sigma_k)\partial_y k &= \epsilon - \nu_t(\partial_y U)^2 \\ \partial_y(\nu + \nu_t/\sigma_e)\partial_y \epsilon &= [C_{\epsilon_2}\epsilon - C_{\epsilon_1}\nu_t(\partial_y U)^2]/T\ . \end{aligned} \tag{5}$$

$C_{\epsilon_1}, C_{\epsilon_2}, \sigma_k$ and σ_e are constants. The left sides of (5) represent turbulent diffusion of energy and dissipation, and the right sides represent the imbalance between destruction and production of energy and dissipation. T is a time-scale, which we take to be

$$T = \max(k/\epsilon, C_T(\nu/\epsilon)^{1/2}) \tag{6}$$

with $C_T = 6$, from DNS data. Away from the wall ($y_+ > 5$ or so), this becomes the Lagrangian decorrelation scale k/ϵ. Because this Lagrangian time-scale tends to zero at the wall, the Kolmogorov scale has been used as a lower bound on T.

A $\overline{v^2}$ model based on usual modeling procedures would be

$$\partial_y(\nu + \nu_t/\sigma_k)\partial_y \overline{v^2} = \frac{\overline{v^2}}{k}\epsilon - \wp_{22}, \tag{7}$$

where $\wp_{22}$ represents the velocity-pressure gradient correlation combined with part of the dissipation. The first term on the right side is an anisotropic contribution to dissipation of $\overline{v^2}$ (see Durbin 1990 for more discussion).

The suppression of $\overline{v^2}$ by the no-normal flux condition (4) is quite important. It is responsible for the behavior shown in figure 1. In order to introduce this boundary condition and the associated homogeneous solutions, we propose an elliptic model for $\wp_{22}$:

$$\begin{aligned} L^2\partial_y^2 f_{22} - f_{22} &= -\Pi_{22} - (\frac{\overline{v^2}}{k} - \frac{2}{3})/T \\ \wp_{22} &= k f_{22} \ . \end{aligned} \tag{8}$$

The second term on the right side of the first equation is associated with dissipation rate. In the homogeneous limit, it will make the dissipation rate isotropic in (7). Π_{22} is a homogeneous pressure strain model. Thus (8) provides for elliptic relaxation to the homogeneous limit. We use the Launder, Reece,& Rodi (1975) form for Π_{22}

$$\Pi_{22} = \frac{C_1}{T}(\frac{2}{3} - \frac{\overline{v^2}}{k}) + C_2\frac{\nu_t}{k}(\partial_y U)^2. \tag{9}$$

L is the length scale

$$L = C_L \max(k^{3/2}/\epsilon, C_\eta(\nu^3/\epsilon)^{1/4}). \tag{10}$$

The elliptic relaxation model is largely justified by the fact that the wall causes irrotational fluctuations in the interior of the flow when the no-normal flux condition is imposed (Hunt and Graham 1978). This is a kinematic effect which cannot be associated with any terms in the Reynolds stress budget. The present representation of these irrotational fluctuations is quite indirect.

Predictions by this model are compared to DNS channel flow data in figures 2 ($R_\tau = 395$) and 3 ($R_\tau = 180$). The predictions are certainly as good or better than those obtained using a damping function to correct the k–ϵ formula (2) (Shih 1990). My hope is that the present approach is more sound.

2.2. Local anisotropy in strained turbulence

In order to obtain the predictions in figure 2, it was necessary to use a higher than usual value of C_{ϵ_1}; in other words, the production of dissipation was higher than in quasi-homogeneous models. A possible source of this extra production of

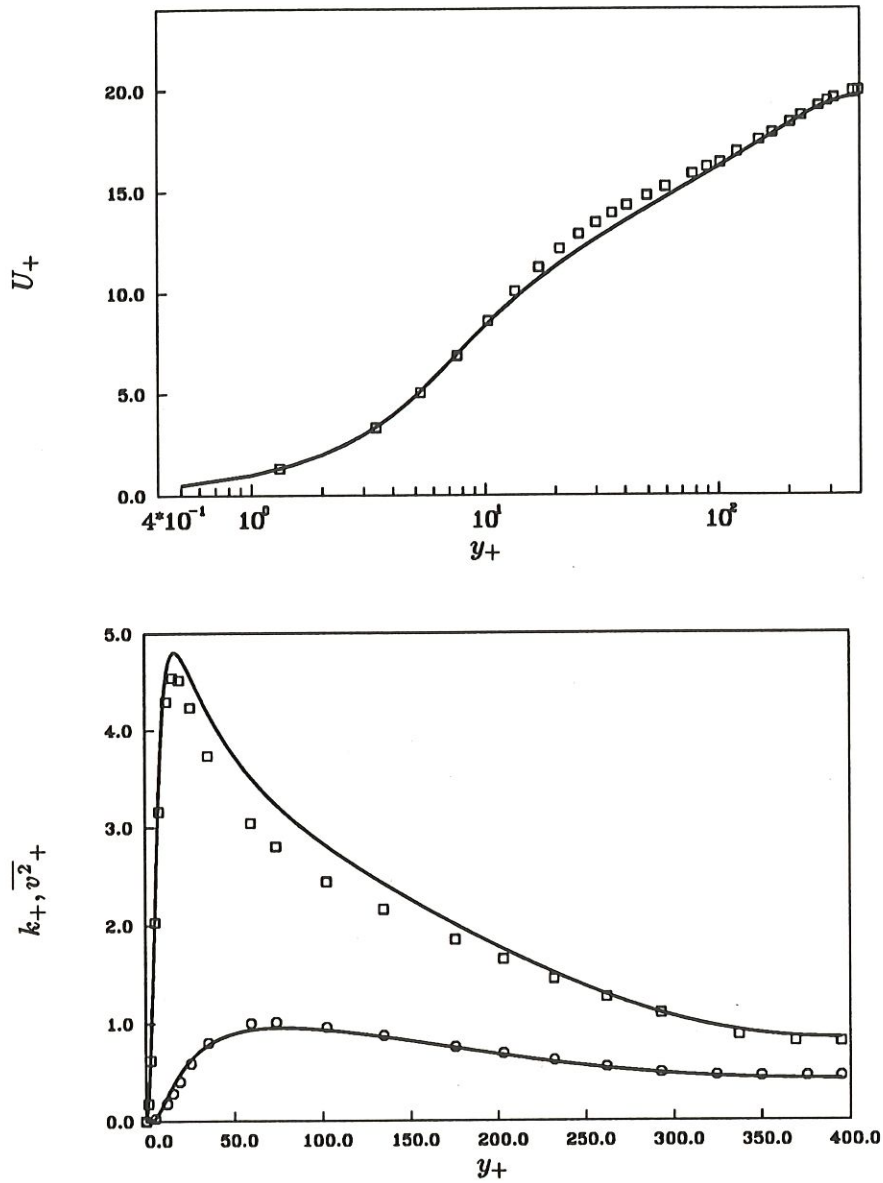

FIGURE 2. $R_\tau = 395$. Comparison of present model (line) to DNS data (symbols): (a) mean flow; (b) k (upper curve) and $\overline{v^2}$ (lower curve).

dissipation is anisotropy of the vorticity tensor. The exact equation for dissipation contains the term

$$(\epsilon_{ij} + d_{ij})S_{ij} \tag{11}$$

with the convention of summation on repeated indices, and where S_{ij} is the mean rate of strain tensor and

$$\epsilon_{ij} = 2\nu\overline{\partial_k u_i \partial_k u_j}, \quad d_{ij} = 2\nu\overline{\partial_i u_k \partial_j u_k}. \tag{12}$$

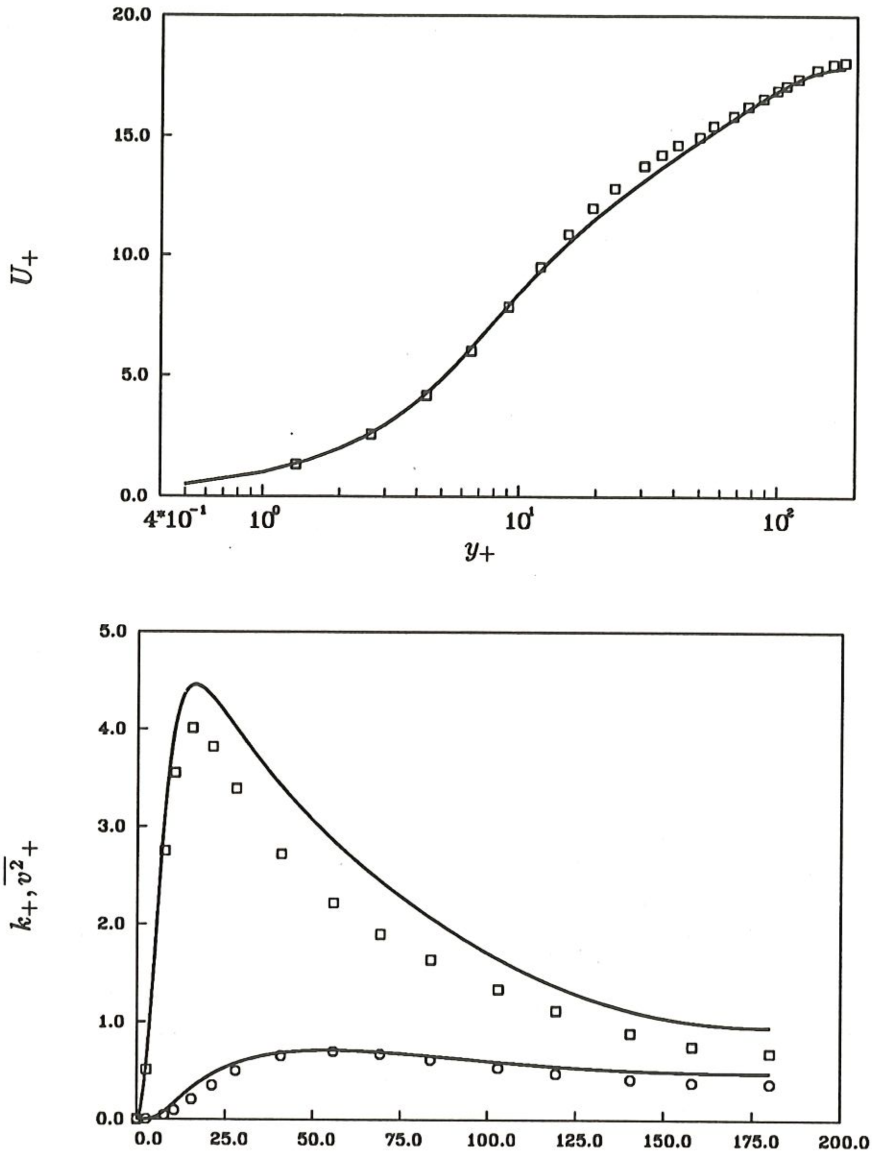

FIGURE 3. $R_\tau = 180$. Comparison of present model to DNS data.

In homogeneous flow

$$\epsilon_{ij} + d_{ij} = -2\nu(\overline{\omega_i\omega_j} - \frac{2}{3}\delta_{ij}\overline{\omega_k\omega_k}). \tag{13}$$

A corollary to the hypothesis of local (or small-scale) isotropy is that $\epsilon_{ij} + d_{ij} = 4\epsilon\delta_{ij}/3$, so that (11) vanishes in incompressible flow ($S_{ii} = 0$).

Although the hypothesis of local isotropy is usually understood to depend on a condition of high Reynolds number, it would also seem restricted to low mean rates of strain. To see this, one notes that in homogeneous turbulence, the equation for ϵ_{ij} is

$$d_t\epsilon_{ij} = N_{ij} + 2(d_{ikjl} + d_{jkil})\partial_l U_k - \epsilon_{ik}\partial_k U_j - \epsilon_{jk}\partial_k U_i - 2d_{klij}\partial_k U_l \tag{14}$$

where

$$N_{ij} \equiv 2\nu\overline{(\partial_i u_j + \partial_j u_i)\partial_k u_l \partial_l u_k} - \overline{\epsilon'_{ik}\partial_k u_j} - \overline{\epsilon'_{jk}\partial_k u_i} - 4\nu^2\overline{\partial^2_{km}u_i\partial^2_{km}u_j}$$

contains the non-linear and dissipative terms and

$$d_{ijkl} = 2\nu\overline{\partial_i u_k \partial_j u_l}.$$

Equation (14) contains only statistics of the velocity gradient tensor, so the hypothesis of local isotropy should apply term by term. Therefore,

$$\begin{aligned} \epsilon_{ij} &= \frac{2}{3}\epsilon\delta_{ij};\ N_{ij} = \frac{2}{3}N\delta_{ij} \\ d_{ijkl} &= \frac{4}{15}\epsilon\delta_{ij}\delta_{kl} - \frac{1}{15}\epsilon(\delta_{ik}\delta_{jl} + \delta_{jk}\delta_{il}) \end{aligned} \tag{15}$$

in which $\epsilon_{ii} = 2\epsilon$ is twice the rate of kinetic energy dissipation, $N_{ii} = 2N$, and $d_{kkij} = \epsilon_{ij}$ has been used. On substituting (15) into (14), one finds

$$\frac{2}{3}\delta_{ij}d_t\epsilon = \frac{2}{3}\delta_{ij}N - \frac{4}{15}\epsilon S_{ij}. \tag{16}$$

Because $S_{ii} = 0$, (16) can only be satisfied if $S_{ij} = 0$; conversely, local isotropy is inconsistent with the Navier-Stokes equations if $S_{ij} \neq 0$. With the conventional estimate $N = O(\epsilon/T)$, the condition for local isotropy to be a valid approximation is that $ST \ll 1$. In the wall region, ST reaches values of about 16. DNS computations show significant local anisotropy in that region.

The ϵ model (5) is not justified by reference to the exact terms which the model replaces; instead, it is based on a loose notion that the difference between production and dissipation of ϵ can be modeled as a function of the production and dissipation of energy. Thus one writes

$$N = \frac{\epsilon}{T}F(P/\epsilon) \tag{17}$$

(N is as in (16) and P means rate of turbulent kinetic energy production). The standard model (5) amounts to assuming a linear form for F; thus

$$N = \frac{\epsilon}{T}[C_{\epsilon_1}P/\epsilon - C_{\epsilon_2}]. \tag{18}$$

The additional production of dissipation by local anisotropy might be incorporated by letting C_{ϵ_1} depend on P/ϵ. Assuming that dependence to be linear amounts to including a quadratic term in F:

$$N = \frac{\epsilon}{T}[C_{\epsilon_1}P/\epsilon\frac{(1 + a_1 P/\epsilon)}{(1 + a_1)} - C_{\epsilon_2}]. \tag{19}$$

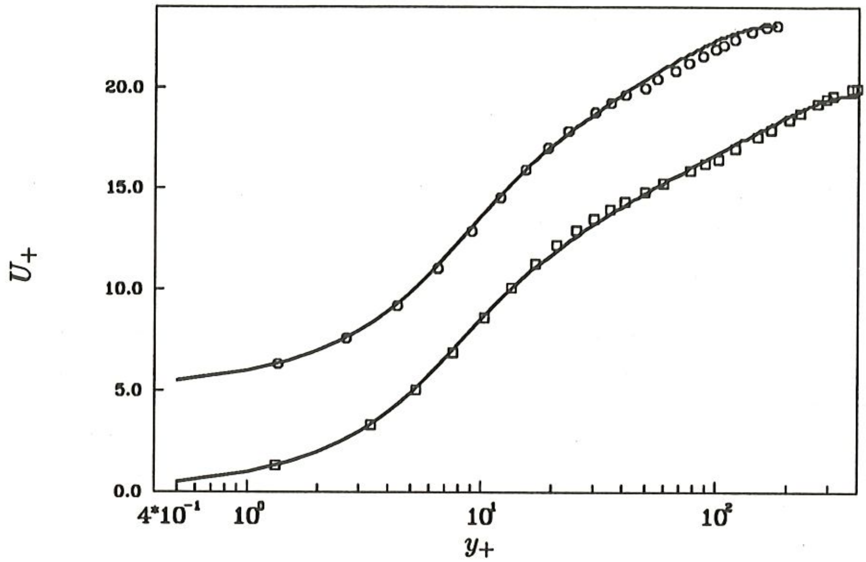

FIGURE 4. Mean velocity profiles with anisotropy term. $R_\tau = 395$ and 180. The upper curve, for which $R_\tau = 180$, has been displaced up by 5 units.

This reduces to (18) when $P = \epsilon$. A computation using (19) in the present near wall model is included in figure 4. Here $a_1 = 0.1$. While one might find this inclusion of an extra constant dissatisfying, the fact is that local anisotropy does contribute significantly to dissipation in the part of the near wall region in which $P/\epsilon > 1$. Thus (19) was chosen because it enhances production of dissipation in the right region and reduces to the standard model in the outer region, where $P \approx \epsilon$.

2.3. k/ϵ is a Lagrangian time-scale

It is useful to have some understanding of the time-scale which enters turbulence models. While $T = k/\epsilon$ might be justified solely on dimensional grounds, I wish to point out that it is also a Lagrangian decorrelation time-scale. Comparison of (3) to the Markovian limit of Lagrangian dispersion theory suggests that it may indeed be appropriate to regard T as a Lagrangian time-scale (after invoking Reynolds' analogy).

When the turbulence is non-homogeneous, Lagrangian statistics are non-stationary so T cannot be an integral scale. Rather, it is a local decorrelation scale in the following sense: The Lagrangian auto-correlation for an ensemble of trajectories originating at y is

$$R_L(y) = \frac{\overline{\mathbf{u}(t;y) \cdot \mathbf{u}(t+\tau;y)}}{(\overline{|\mathbf{u}(t;y)|^2}\ \overline{|\mathbf{u}(t+\tau;y)|^2})^{1/2}}. \tag{20}$$

By Kolmogorov scaling

$$R_L = 1 - c\epsilon\tau/k + O(\epsilon\tau/k)^2, \quad \tau_\eta \ll \tau \ll T$$

where c is a constant. Define T by

$$\frac{1}{T(y)} = \lim_{\tau/T \to 0} \frac{1 - R_L}{\tau}. \tag{21}$$

(The limit is asymptotically equivalent to $\tau/\tau_\eta \to \infty$.) One finds that $T \propto k/\epsilon$. Hence, k/ϵ is a Lagrangian decorrelation time-scale.

3. Future plans

A primary motivation for developing near wall models is the need to predict non-equilibrium boundary layers, especially those approaching separation. My hope is to extend the present efforts into that direction. Such work on boundary layers has already begun. The present near wall model appears to be satisfactory. However, the rotational-irrotational interface seems to be a source of difficulty. Irrotational fluctuations contribute to the turbulent energy in the outer part of the boundary layer. Again, the irrotational 'action at a distance' cannot be identified with any term in the Reynolds stress budget (it is *not* an effect of pressure-strain correlation). Near the wall, the dominant effect of these irrotational fluctuations was to suppress the normal velocity. In the outer half of the boundary layer, they contribute to the total kinetic energy. This problem is under investigation. A parabolic code with an expanding grid was written for this work. Ultimately, it will be necessary to write a fully elliptic code. Use can be made of DNS techniques.

REFERENCES

DURBIN, P. A. 1990 Near wall turbulence closure modeling without 'damping functions'. *CTR Manuscript 112,* Center for Turbulence Research, Stanford University.

HUNT, J. C. R. & GRAHAM, J. M. R. 1978 Free-stream turbulence near plane boundaries. *J. Fluid Mech.* **84**, 209-235.

LUMLEY, J. L. 1978 Computational modeling of turbulent flows. *Adv. Appl. Mech.* **18**, 126-176.

LAUNDER, B. E., REECE, G. J. & RODI, W. 1975 Progress in the development of a Reynolds-stress turbulence closure. *J. Fluid Mech.* **68**, 537-566.

SHIH, T.-S. 1990 An improved k–ϵ model for near wall turbulence and comparison with direct numerical simulations. Unpublished.